A Computational Framework for Breast Surgery Application to Breast Conserving Therapy

David Thanoon[+], Marc Garbey[+], Nam-Ho Kim[++], and Barbara Bass[+++]

Abstract Breast conserving therapy (BCT) comprised of complete surgical excision of the tumor (partial mastectomy) with post-operative radiotherapy to the remaining breast tissue, is feasible for most women undergoing treatment for breast cancer. The goal of BCT is to achieve local control of the cancer as well as to preserve a breast that satisfies the woman's cosmetic concerns. While most women undergo partial mastectomy with satisfactory cosmetic results, in many patients the remaining breast is left with major cosmetic defects including concave deformities, distortion of the nipple areolar complex, asymmetry and changes in tissue density characterized by excessive density associated with parenchymal scarring. There are currently no tools, other than surgical experience and judgment, that can predict the impact of partial mastectomy on the contour and deformity of the treated breast. The objectives of this study are to determine if a computational model can allow prediction of the breast contour, surface features and tissue density after partial mastectomy and potentially identify targets for intervention to improve cosmetic results. This chapter is a preliminary study. The aim is to start from the simplest model and build on complexity until we obtain a model that can add value in surgery planning.

1 Problem and Motivation

1.1 Introduction

If a surgical intervention is needed, early stage breast cancer may lead to three basic surgery choices: breast-sparing surgery followed by radiation therapy, mastectomy,

(+) Department of Computer Science
(++) Department of Mechanic and Aerospace Engineering University of Florida
(+++) Department of Surgery at The Methodist Hospital and Weill Medical College of Cornell University

mastectomy with breast reconstruction surgery. Breast-sparing surgery (Breast Conservation Therapy - BCT -) removes the breast tumor and a margin of surrounding normal tissues. It is also known by other names: lumpectomy, partial mastectomy, segmental mastectomy and quadrantectomy. Radiation therapy follows lumpectomy to eliminate any microscopic cancer cells in the remaining breast tissue. The purpose of BCT is to give women the same cure rate they would have if they were treated with a mastectomy but to leave the breast intact, with an appearance and texture as close as possible to what they had before treatment. Trials for breast conservative therapy with patients affected by breast cancer (I and II) have demonstrated conclusively that BCT produces disease control and survival rates at least equivalent to those of mastectomy, and possibly better in the long run for patients with stage II [8]. BCT is combined to radiation therapy. While BCT removes the tissue that contain the tumor with a negative margin, radiotherapy insure that residual microscopic disease are controlled. Contra-indications to BCT is generally for patients with high probability of recurrence, high probability of normal tissue damage from irradiation. While cosmesis after BCT might be generally satisfactory, the quality of the result is very sensitive to the location and extend of the tumor. Further the breast is a very deformable structure with a complicated anatomy that is patient specific. The mechanical properties of glandular, fatty and cancerous tissue are quite different, and vary from one patient to another. The Cooper's ligament play also a key role in the outcome. Strong asymmetry in the location or large tumor size are prone to anesthetic BCT result. Surgical results are also depending on the time scale. Beside the short time scale modeling that might be caught by the mechanical model, one can expect that inflammation, post-surgical radiotherapy and healing dynamic can change significantly in the long time scale the cosmetic outcome. In other words biology plays a role as well.

The same way that it takes a multidisciplinary team, involving a surgeon, a radiologist, an oncologist etc... to manage a breast cancer, it takes a multidisciplinary model involving soft tissue mechanic, medical imaging and biology modeling to predict the outcome of BCT. The objectives of this study is to construct a modular computational model that can allow the prediction of the breast surface contour, after partial mastectomy and potentially identify targets for intervention to improve cosmetic results. Key questions are:

- a priori model of the breast deformation in order to be able to define the pattern of cosmetic defects for women undergoing BCT with numerical simulation.
- to determine if patterns of deformity can be predicted based on preoperative imaging and surgical data points.

The philosophy of this preliminary study is to develop a computational framework that can feed on a cost effective clinical protocol and help significantly surgery planning with BCT. We do not look for a perfect model but rather a useful model.

We are going first to review the individual models that are available in the literature.

1.2 Model and Related Work

There have been a large stream of work on patient specific bio-mechanical models of the breast used to predict deformation [17]. The goal of such studies is to compute the change in shape as external mechanical forces are varied. The standard application is co-registration of internal structure of interest such as tumors. We are going to see that this soft tissue mechanical problem by itself is fairly difficult to solve. While the surgical intervention is typically with the patient lying on his back, pre-surgery planning relies on medical imaging with different positions. The breast is a highly deformable organ fairly sensitive to gravity load. For MRI the patient lies prone and the breast is allowed to drop under gravity. The prone position is not particularly inherent to the MRI procedure, but rather to the available existing equipment. It is unfortunate that these MRI images cannot be directly used to surgery but should rather be transformed to accurately track the tumor location. For x-ray, the subject stands and the breast has to be pressed between two plates. Under such conditions it is critical to compute an accurate registration of the tumor that can localize the tumor in the absence of external pressure. Registration should be much improved if one use a bio-mechnical model to predict the tumor location as a function of the gravity load. The problem of an accurate registration of the tumor location is also seen in biopsy, because the needle is not a very sharp object. A straight trajectory may result in fact into a trajectory that changes direction at the interface between different layers of tissues. Overall the biopsy may not collect the targeted tissue sample. There is a large number of papers on the prediction of mechanical deformation of the breast that started with the extensive use of Finite Element Models (FEM) [1, 16, 20]; two papers of particular interest are the Medical Image Analysis article of F.Azar, D. N.Metaxas and M.Schnall [2] that concentrates on the biopsy application and emphasis the link between the model and image analysis, and the article of V.Rajagopal, J.H. Chung, D.Bullivant, P.M.F.Nielsen and M.Nash in the Inter. J.of Numer. Meth. Engng [14] that discusses the problem of the reference state. Both papers have pretty extensive bibliographies. In Azar et Al work, a custom written program for the image segmentation of the 3D breast is linked to the ABAQUS model. Image segmentation of the breast should at least take into account the two predominant types of tissue that are fat and normal glandular tissue. Image segmentation of the tumor should be added for BCT.

There is a fair amount of uncertainty in material properties of the soft tissue that compose the breast. Further such properties are very much patient specific. According to Krouskop et Al [12] fat tissue and glandular tissue have similar elastic modulus at low strain levels, while glandular tissue elastic modulus increases by one order of magnitude at high strain levels. Further fibrous tissue have an elastic modulus one to two order of magnitude higher than fat tissue. In [2] the breast fatty tissue model takes also into account the effect of fat compartmentalization due to Cooper's ligament. Finally tumor tissues are much stiffer than surrounding tissue as measured for example in [13].

Actually skin mechanical properties might also be taken into account separately and modeled possibly as a two dimensional deformable shell that bounds the 3D

model. Further it might be difficult to predict the right boundary conditions that describes the attachment of the breast to the muscle of the thorax. For all these reasons, while the validation of the FEM with a phantom study using a deformable silicon gel is kind of reassuring, the FEM still needs to be validated with patient as in [2, 15]. Most previous studies of breast modeling deformations have been conducted for large deformation due to mammographic compression or for biopsy. Most of these studies were conducted using Moonley-Rivlin Hyperelastic models under large deformation. Still small deformation theory has been used thanks to either a continuation method or time stepping but requires then to control the accumulation of errors from each step. In many of these studies, the computation of the mechanical model was verified by comparison with experimental data on gel phantoms that have very similar properties to breast tissue. Comparison to clinical data is however sparse and/or involves very few human subjects. One additional difficult problem is that one cannot recover directly the unloaded shape of the breast. Rajagopal et Al [14] have shown that the accuracy of shape prediction is much improved by recovering a stress free unloaded position virtually. In this work Rajagopal et Al propose a numerical algorithm to solve that inverse problem, and use a special experimental set up to validate that study with human subjects. One still needs to assume that the unloaded shape is free of stress which is fairly unclear in particular for breast cancer. Though most of these studies reported here considered the breast tissue as incompressible isotropic homogeneous, no study, as far as we know, was focussed on BCT.

Realistic tumor dynamic modeling is very challenging as well. For BCT one is interested on tissue margin, i.e how much of the tissue BCT should take away, and possibly how one make sure that chemotherapy and/or radiotherapy can control what might be left of cancer cells in the breast. There is a vast literature on model and simulation of tumor growth. The chapter from T. Colin et Al in this book concentrates on a multi-scale PDE model representative of the state of the art. Cellular Automata (CA) [21] and/or Agent Base Model (ABM) [10] might be used as well to simulate the dynamic of the population of cells involved in cancer [5], in particular in situation with sparse density of tumor cells. Both CA and ABM techniques belongs to the bottom up approach where individual cells behavior and interaction with their environment are explicitly modeled. One can observe a posteriori in the simulation the emerging dynamic of the complex system. Implementation of these methods has been reviewed recently in [11]. These methods can be applied to tumor dynamic as well as modeling inflammation and tissue healing [3, 6, 19, 9, 7]. The limit of such model is the inherent complexity of the biological environment and the difficulty to capture adaptation and mutation of individual cells.

However the future is to design multi-scale hybrid model that can couple the mechanical description of tissue with the long time scale dynamic of the biological tissue that is essential to recovery [4]. The challenge, indeed, is to have patient specific model that can be used in clinical conditions and that can feed on existing data acquisition processes such as tissue elastography for tissue mechanical properties and biopsy for cell population.

We are going now to discuss various computational methods to simulate the mechanical deformation of the breast. We will report in this chapter exclusively on artificial benchmark problems to develop the computational methods. Image based simulation with patient data will be reported elsewhere.

2 Model of Mechanical Deformation of the Breast

Typically a mechanical model requires the description of the material properties of the breast along with anatomic data, an initial state and some boundary conditions.

The model can be either static, i.e describe an equilibrium, or dynamic, i.e describes the time dependent deformation. Further the model can incorporate the material properties of the tissue with a wide range of level of details.

We are going to review our experiment with several models with increasing level of complexity. We will assume that we start from a known shape at zero gravity conditions and with zero internal stress. The solution of our benchmark problem is the displacement and stress distribution for the equilibrium position at standard gravity. All simulations here are implemented with the commercial software COMSOL MULTIPHYSICS^{TM} [23]. COMSOL is a software based on finite element approximation that allows fast prototyping.

For simplicity our benchmark problem is a semi-sphere attached to the wall as in figure 1. This simplified benchmark problem will be used to compare linear and nonlinear models, and will be enough to show some limitation of the simulation. We start with the standard linear elasticity model.

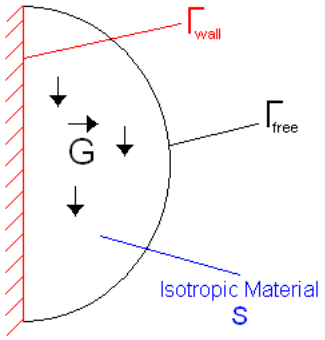

Fig. 1 Geometry of the benchmark problem

2.1 Linear Elasticity

Let us start with the small deformation theory that is implicitly assumed in the linear elasticity model that will help understanding further refinement in the modeling:
The unknown of the mechanical problem is the field:

$$\left(\overrightarrow{u}\left(\overrightarrow{x}\right),\overline{\overline{\sigma}}\left(\overrightarrow{x}\right)\right),\forall\overrightarrow{x}\in S \tag{1}$$

in the semi-sphere S with $\overrightarrow{u}\left(\overrightarrow{x}\right)$ representing the displacement, $\overline{\overline{\sigma}}\left(\overrightarrow{x}\right)$ representing the engineering stress.

It is possible to completely describe the strain condition at a point with the deformation components u_i for $i=1,2,3$ and their derivatives. The strain components are given from the deformation as follows:

$$\varepsilon_{ij}=\frac{1}{2}\left(\frac{\partial u_i}{\partial x_j}+\frac{\partial u_j}{\partial x_i}\right) \tag{2}$$

Also, the stress-strain relationship for a linear isotropic material reads:

$$\overline{\overline{\sigma}}=\lambda\left(tr\overline{\overline{\varepsilon}}\right)\overline{\overline{I_3}}+2\mu\overline{\overline{\varepsilon}}\ ,\quad \forall\overrightarrow{x}\in S \tag{3}$$

with λ and μ the elasticity coefficient of Lame linked to E, the modulus of elasticity (known as *Young's modulus*), and ν *Poisson's ratio* by:

$$\lambda=E\frac{\nu}{(1+\nu)(1-2\nu)}\ ,\qquad \mu=\frac{E}{2(1+\nu)} \tag{4}$$

Under static conditions, the equilibrium equations writes:

$$div\overline{\overline{\sigma}}+\rho\overrightarrow{g}=\overrightarrow{0} \tag{5}$$

where $\overrightarrow{g}$ denotes the body forces per mass.
The Boundary Conditions are the following:
For the embedment: $u_i\left(\overrightarrow{x}\right)=0\ ,\quad \forall\overrightarrow{x}\in\Gamma_{wall}$
For the free surface: $t_i\left(\overrightarrow{x}\right)=\sigma_{ij}\left(\overrightarrow{x}\right)n_j\left(\overrightarrow{x}\right)=0\ ,\quad \forall\overrightarrow{x}\in\Gamma_{free}$
With $\Gamma=\Gamma_{wall}\cup\Gamma_{free},\quad \Gamma_{wall}\cap\Gamma_{free}=\oslash$
where the $n_j\left(\overrightarrow{x}\right),(j=1,2,3)$ are the components of the outward unit normal vector $\overrightarrow{n}\left(\overrightarrow{x}\right)$

Instead of using directly this formulation, to extend the small deformation theory to the large deformation situation we use time stepping with the adaptive time step provided by COMSOL, and increase the gravity progressively from zero at initial stage to g in a physical time of 60 s.

We suppose that the tissue is an linear isotropic material with *Young's Modulus* $E=2520\ Pa$ and a *Poisson's ratio* $\nu=0,4$ [22]. The simulation is completed with 17000 Quadratic Lagrange Elements. The static solution is shown in figure 2.

Figure 2 shows the von Mises stress: a singularity appears near the corner of the

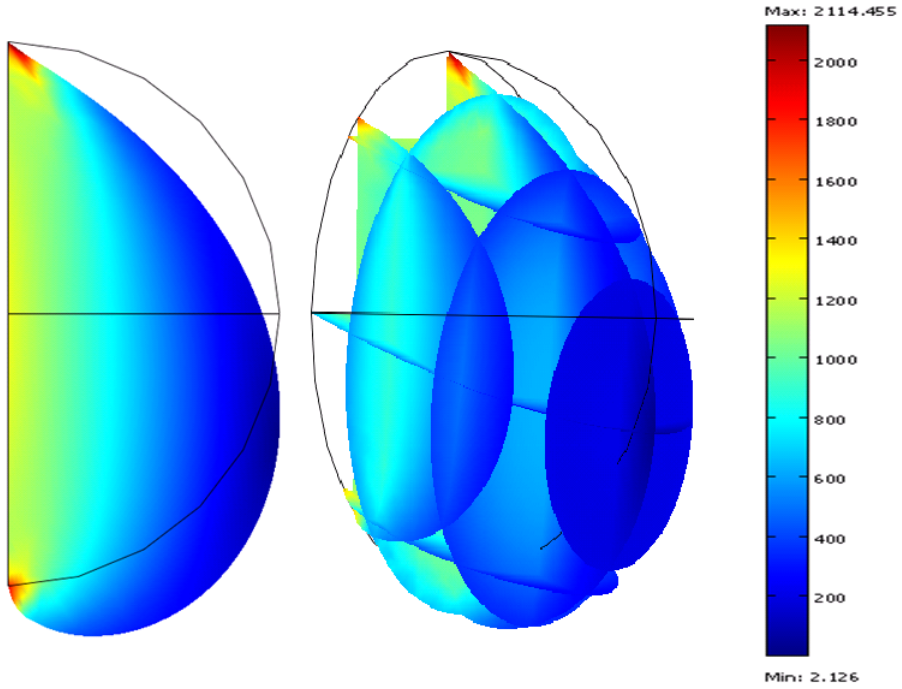

Fig. 2 Deformation of the single 3D isotropic breast model under the gravity, plotting the von Miss stress [Pa]($E = 2520\ Pa\ , \nu = 0,4$)

.

breast. This singularity appears to be an artifact due to the non-realistic boundary condition imposed at the "wall".This problem should be avoided by choosing a new geometry model that includes the body core. We provide more realistic boundary conditions next by adding a wall support as in figure 3. Regardless of this singularity, the breast static state has some analogy with good shape of a healthy women breast.

The next step was to simulate the breast state after a surgical intervention of the breast with the removal of cancerous tissue. This surgical intervention was modeled with the introduction of a small sphere $S_{removal}$ with a radius $R_{interior} = 3cm$ inside the semi-sphere - see Figure 3 (Material 2). We suppose that after the surgical intervention this empty part will be first filled up with a liquid.

Model I: We approach the liquid properties material by choosing a water density $\rho = 1000kg.m^{-3}$ a small *Young's Modulus* $E = 300\ Pa$ and a *Poisson's ratio* $\nu =$

$0,495$ since only the mass contribution of the fluid during the analysis is of interest. Simulation results are shown in figure 4 .

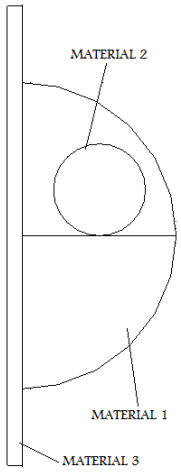

Fig. 3 Geometry of the post-surgery breast model

.

This simulation still exhibit a singularity near the wall due to the change in material properties at the interface between material 2 and 3. We observe the impact of tissue removal on the overall shape of the breast. A bump appears which gives a non-conform shape to the breast. Our modeling of tissue removal is fairly naive and the modeling of water can be interpreted in a more physical way.

Model II: To model water in COMSOL we use an anisotropic material with a singular representation of the elasticity matrix. The stress-strain relationship for an anisotropic material is linked by the following relation $\sigma = D\,\varepsilon$ where D is the 6-by-6 elasticity matrix and the stress and strain are both given in column vector form:

$$\begin{pmatrix} \sigma_x \\ \sigma_y \\ \sigma_z \\ \tau_{xy} \\ \tau_{yz} \\ \tau_{xz} \end{pmatrix} \textit{and} \begin{pmatrix} \varepsilon_x \\ \varepsilon_y \\ \varepsilon_z \\ \gamma_{xy} \\ \gamma_{yz} \\ \gamma_{xz} \end{pmatrix}$$

Water is supposed to be a perfect fluid, with no friction, indeed the only permissible load is the hydrostatic pressure, volumetric force. In order to avoid the friction force the elasticity matrix is divided in 4 smaller 3-by-3 matrix where the 3 blocs that are in relation with the friction effect, τ_{**}, are equal to zero. Since only the hydrostatic pressure force occurs it can be represented by the relation with the bulk modulus. Indeed the bulk modulus of a fluid measures the fluid resistance to uniform compression. It is defined as the pressure increase needed to effect a given relative decrease in volume. The bulk modulus K can be formally defined by the

equation: $K = -V\frac{\partial P}{\partial V}$ where P is the pressure, V is the volume, and $\frac{\partial P}{\partial V}$ denotes the partial derivative of pressure with respect to volume. The inverse of the bulk modulus gives a substance compressibility. This relation can be arranged as the following $K\frac{\partial V}{V} = -\partial P$. By analogy on mechanic basic we can state that $\sigma = -\partial P$ and that $trace(\varepsilon) = (\varepsilon_x + \varepsilon_y + \varepsilon_z) = \frac{\partial V}{V}$. This leads to an elasticity matrix with the following form:

$$D = \begin{pmatrix} K & K & K & 0 & 0 & 0 \\ K & K & K & 0 & 0 & 0 \\ K & K & K & 0 & 0 & 0 \\ 0 & 0 & 0 & 0 & 0 & 0 \\ 0 & 0 & 0 & 0 & 0 & 0 \\ 0 & 0 & 0 & 0 & 0 & 0 \end{pmatrix}.$$

The result of this simulation is illustrated in figure 4, where it shows von Miss stress of the meridional cut of the breast. This simulation was done with the same elastic linear model than before and the value of the water bulk modulus $K = 2.2e9\ Pa$. In comparison with the first water model we can see that in our second model the value of the stress inside the liquid is equal to zero whereas in the first model the liquid has some stress. We can assume that our second model is more realistic and gives a more physical result. However we can see that in the two models the bump and the exterior shape are quite similar.

The material property chosen for the model so far was linear isotropic. This is not the true mechanical properties of soft tissue. Indeed the stress-strain relationship of breast tissue is hyperelastic.

2.2 Towards a non-linear modeling

The breast often deforms significantly, linear elasticity with the infinitesimal deformation formulation is not appropriate to formulate the breast model. As a result we used a finite deformation formulation in conjunction with hyperelastic material.

The problem is to find the coordinates ($\mathbf{x}$) of the deformed body, V, given the coordinates, ($\mathbf{X}$) of the undeformed body V_0. the deformation gradient tensor $\mathbf{F}$ provides the relationship to map between the undeformed states, and is defined as

$$\overline{\overline{F}} = \left\{ \frac{\partial x_i}{\partial X_M} \right\} \tag{6}$$

The Green Lagrange strain tensor $\mathbf{E}$ is calculated using:

$$\overline{\overline{E}} = \frac{1}{2}\left(\overline{\overline{F}}^T\overline{\overline{F}} - \overline{\overline{I}}\right) \tag{7}$$

The aim is to find a solution vector $\overrightarrow{x}$ representing the degrees of freedom defining the deformed state, such that the principles of conservation of mass, linear momentum, and angular momentum are satisfied. The modeling framework has been

expressed with respect to the reference configuration and thus the equations below are written in terms of the undeformed state. The reason is that we do not know the deformed shape since we are dealing with large deformation.

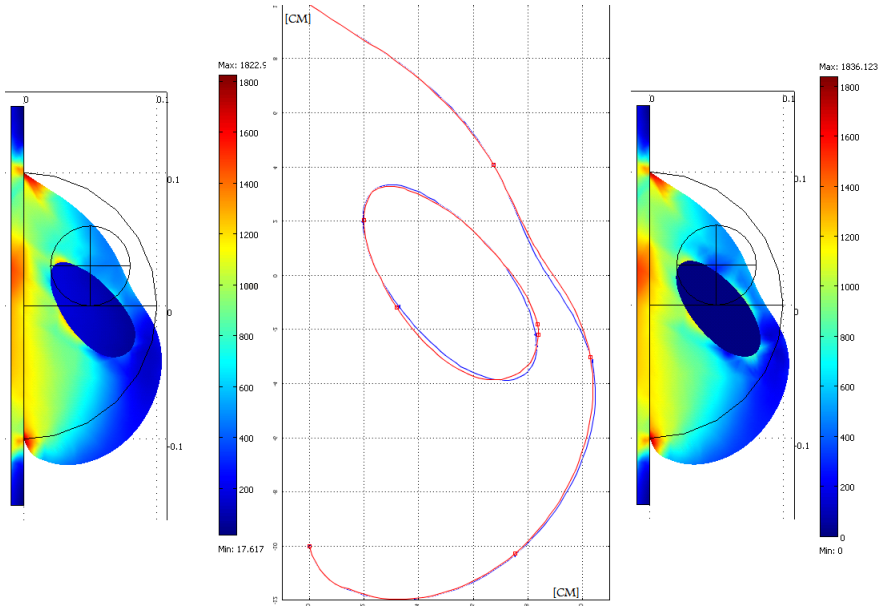

Fig. 4 Von miss stress and deformation of the breast model with tumor removal using: (left) water model I [min 17 Pa;Max 1822 Pa] ; (right) water model II [min 0.Pa;Max 1836 Pa]; (middle) Comparison of breast and tumor removal deformation for water model I (red), and water model II (blue)

Fig. 5 Plot of the time dependent gravity load $\times 10\, m.s^{-2}$

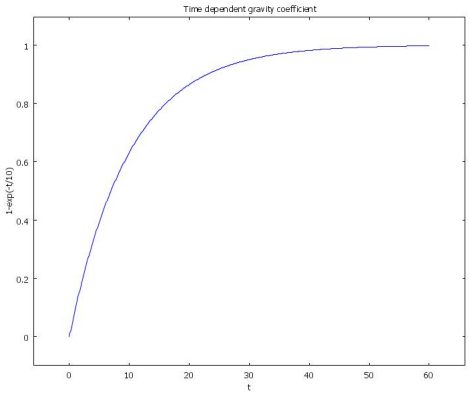

.

When a body is in equilibrium, all of the forces must balance. This is achieved by satisfying the principle of conservation of linear momentum that can be written for a static problem as:

$$\frac{\partial}{\partial X_M}\left(S^{MN}\frac{\partial x_j}{\partial X_N}\right)+\rho_0 f^j=0, \tag{8}$$

where S^{MN} are components of the second Piola Kirchhoff stress tensor (force per unit area of the undeformed body) and f_j are the body forces in the reference frame(such as gravity in our problem).
We model the breast tissue as a Hyperelastic material which is a material where the stresses are computed from a strain energy density function. It is assumed that the Second Piola-Kirchhoff stresse $\overline{\overline{S}}$ is used, so that

$$\overline{\overline{S}}=\frac{\partial W_S}{\partial \overline{\overline{E}}}$$

For an isotropic material the strain energy function, W_S, can only be a function of the strain invariants. In a total Lagrangian formulation it is convenient to use the right Cauchy-Green tensor $\overline{\overline{C}}=\overline{\overline{F}}^T\overline{\overline{F}}$ for the representation of the strain. Hence the invariants are:

$$I_1=trace(C)=C_{11}+C_{22}+C_{33} \tag{9}$$

$$I_2=\frac{1}{2}(I_1^2-trace(C^2)) \tag{10}$$

$$I_3=det(C)=J^2 \tag{11}$$

where $J=det\,(\mathbf{F})$. We used Mooney Rivlin strain energy, with no thermal expansion, to model breast tissue, it is defined as:

$$W_S=C_{10}(-3+J^{-\frac{2}{3}}I_1)+C_{01}(-3+J^{-\frac{4}{3}}I_2)+\frac{\kappa}{2}(J-1)^2, \tag{12}$$

where C_{10}, C_{01} and κ are the material constants of the breast tissue, these constant units are *Pa*. The value of the material constants C_{10} and C_{01} for the breast tissue are to be determined experimentally. κ is the bulk modulus and carries the volumetric part that represents the resistance to hydrostatic compression. Therefore the higher κ is the more incompressible is the material.

The simulations are done for a static problem. We set the value for the material constants to be $C_{10}=3740\ Pa$ and $C_{01}=1970\ Pa$; these values correspond to a material that is a silicon gel [2]. The first computation was made with a 14000 Quadratic Lagrange Elements. This computation appears then to diverge while we checked that this was not an issue with mesh refinement. An easy solution is to compute the solution of this nonlinear problem as the end result of a transient problem with increasing gravity load as in Figure 5. Alternatively we can stay within the

small deformation theory by artificially increasing the gravity field form zero to the standard value. This continuation method has two advantages: for each step it keeps the strain below the small deformation criteria (strain under 4%) and it enable us to get a solution that converges for each step. Keeping small deformations between each step leads to fast computation. However this method could lead to an accumulation of discretization errors. This method could be seen as a quasi-static method. In our simulation we have increased the gravity for each step by 0.3% of the real gravity value. This means that after 333 incremental steps we can reach the real gravity load. The result of this simulation is shown in figure 6. We can see no singu-

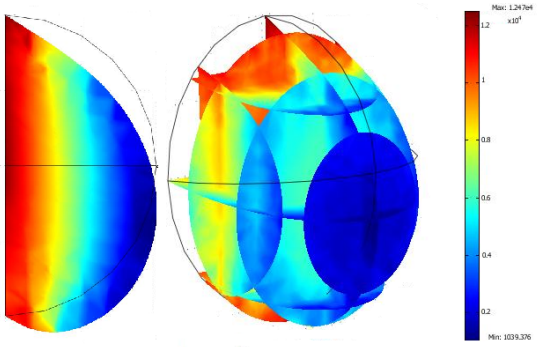

Fig. 6 Simulation of the deformation of the 3D breast model under the gravity using hyperelastic model and the 'quasi-static' method, plotting the von Miss stress [Max=1.24e4 Pa; Min=1039 Pa]

.

larity at the corner and the von Miss stress is continuous. Nevertheless the value of the stress is much higher than the linear elastic model. Although hyperelasticity and linear elastic model are not the same there exists some connection. Indeed for low strain hypothesis (strain $< 5\%$) one can express the relationship between C_{01}, C_{10} and E. The material properties of silicon gel we use, did not allow us to link these two models. Also more validation and verification against experimental data need to be done to validate the model.

2.3 Influence of Poisson ratio

One of the main difficulties with the breast mechanical model is the lack of initial conditions, i.e the fact that no shape under zero load is available. A naive approach will be to start from the loaded configuration, reverse the gravity and expect that this will be the initial shape at zero gravity.

One of the reasons for which this idea does not work, beside the fact that the loaded configuration is not stress free, is that the standard linear elasticity model does not even conserve the volume. In the elastic linear equation the poisson's ratio ν represents the incompressibility of a material. Indeed when a sample of material is stretched in one direction, it tends to contract (or rarely, expand) in the other two

directions. The Poisson's ratio, ν, is a measure of this tendency. The influence of the poisson's ratio can be shown by a two step method. First we apply to our initial geometry a gravity load in a direction, e_z, and we obtain the geometry of the breast under a gravity load. The second step consists in extracting the deformed geometry under gravity and in applying a gravity load in the opposite direction, $-e_z$. After the first deformation the volume changes, hence the integration of the volumetric forces for our deformed geometry differs from the original if we apply the same body force.

However if our model were correct we should obtain after the second step the exact same initial geometry. In order to see the influence of ν, we apply this two step procedure, for different value of ν. The Poisson ratio for materials stands between -1 and 0.5. The value of $\nu = 0.5$ representing the complete incompressibility cannot be reached according to (4). One compute the percentage of the relative error in L_2 norm for the meridional plan of the breast as a function of the second gravity load (in the inverse direction) for different values of ν. We observe that the closer ν is to 0.5 the smaller the error but this error is no less than 2% at minimum. A remedy to that lack of volume conservation would be to constraint the model with a Lagrange multiplier. We are going now to discuss an algorithm to solve the inverse problem that consists in the reconstitution of the initial unloaded shape from a loaded configuration.

2.4 Retrieving the unloaded shape

For simplicity we restrict ourselves to a two dimensional case.

Let us consider a curve $C_{med}(t) = (\theta_{med}(t), r_{med}(t))$ define for $t \in [0, \pi]$, that represents the $2D$ breast external envelop under gravity loading. This parametric representation is done in the polar coordinate system. Our goal is to find the curve $C_s(t) = (\theta_s(t), r_s(t))$ representing the breast model under zero gravity load. When we apply the gravity load to C_s we should obtain C_{med}.
We consider a set of N_c points : $t_1 = 0 < t_1 < ... < t_{N_c} = \pi$ to support a B-spline representation c_s of our unknown contour curve C_s. Our optimization problem in this finite approximation space is summarized in figure 7.

The optimization algorithm is an iterative process that requires an initial guess C_0. We build the initial guess by applying the gravity load in the inverse direction on C_{med}. We may apply a surface rescaling to impose the surface area to be preserved. After construction of our initial guess we compute the loaded shape with one of the previous forward model and compare our controlling points to the medical shape, C_{med}. The controlling points position are updated with an optimization algorithm that minimizes the distance between the two curves. If the tolerance condition is met, the optimization process is terminated. This occurs when the sum of differences between the medical shape and the FEM shape is sufficiently small. Our first attempt to use a gradient based method fails, because this method appears to be too

sensitive to the noise of the forward FEM calculation. Second we use a Nelder-Mead method, that turns out to be more stable and provided convergence. We found more efficient to use some kind of a local relaxation technique that sweep the parameter space and solve the optimization problem one component at a time. This simple algorithm is described as follows:

Until convergence criteria is met repeat the sweeping algorithm:
for $i = 1 : N_c$
$-$ *Optimize position of point i in* C_0*;*
$-$ *Set the new* C_0 *with the optimize position of point i;*
end for

This procedure converges faster with the following regularization that consists to update the two neighbor points with a spline interpolation from the other fixed point and the i^{th} perturbed point.

A representative example of our numerical results was for example with the benchmark problem corresponding to the shape define in the Cartesian coordinates by $(X(t),Y(t)) = (R_0 cos(t), -R_0 sin(t) + X(t))$. The inverse problem requires 1200 forward simulation with 20 control points which is a fair amount of calculation. The relative error expressed in the L_2 norm on the coordinate of the control points was equal to 0.73%. The larger the number of control points the smaller should be this error. To solve efficiently this inverse problem in three space dimension will undoubtedly benefit from a parallel version of the sweeping algorithm that exploit

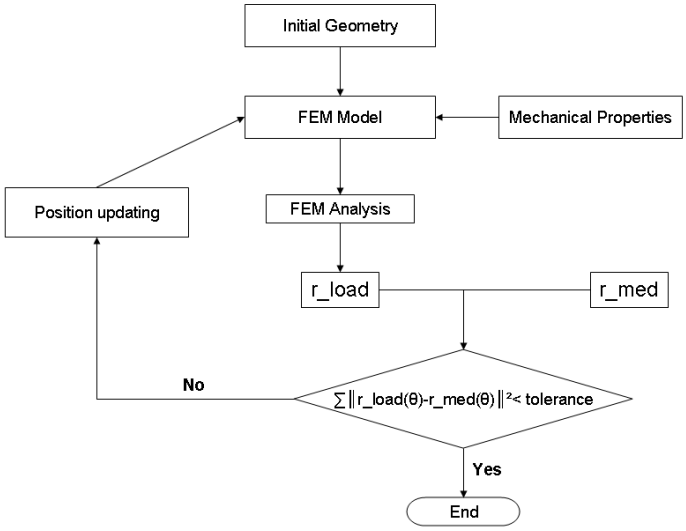

Fig. 7 Optimization algorithm flowchart used to determine the unloaded shape of a breast from a loaded shape

.

the relative independence of distanced control points. This work is under development for 3d clinical cases that are necessary to provide a validation of the method. This reconstruction of the unloaded shape must be done only once. From that result a forward simulation with arbitrary direction of gravity can be done very quickly. However as mentioned earlier there is a fair amount of uncertainty on mechanical soft tissue properties with clinical situation. We are going next to explore the sensitivity of the forward simulation to material properties.

2.5 Influence of Tissue Description

We are mainly concerned by how important is the geometric distribution of soft tissue mechanical properties and what is the impact of internal stiffer tissue on the whole deformation.

To tackle this question, let us consider a $2D$ breast model with a realistic distribution of tissue. The geometry of the breast, as well as the tissue distribution is given in figure 8.

We differentiate three types of tissue: fat, fibroglandular, skin. The individual tissue types were modeled as isotropic and homogeneous. Linear elastic model was used, and we tested a broad variety of Youngs modulus ratios for each tissue types as in table 1), compatible with data find in the literature. Six linear models were

Table 1 Youngs modulus E of fatty and fibroglandular tissue for linear

Young's modulus E in Pa			
Name	Fatty tissue (E_f)	Fibroglandular tissue (E_g)	$\frac{E_f}{E_g}$
MM1	2500	2500	1
MM2	2500	3750	1.5
MM3	2500	12500	5
MM4	2500	25000	10
MM5	2500	37500	15
MM6	2500	50000	20

constructed where fibroglandular tissue was $1, 1.5, 5, 10, 15$ or 20 times stiffer than fatty tissue. These six models were tested without skin $(MM1 - MM6)$, and with skin. The skin envelope was supposed to be 4 times stiffer than the fatty tissue in the linear models $(MM1S - MM6S)$. We start from a loaded configuration with the person standing up. To test our model we apply a body load $\| \overrightarrow{g} \| = 9.8 m.s^{-2}$ in the upward $\overrightarrow{y}$ direction. This would correspond to the position of the breast at zero gravity. The deformation of the breast was monitored by plotting the displacement of five markers attached to the breast. Figure 9 illustrates the displacement of the 5 markers, placed on the breast model (see figure 8), along the $\overrightarrow{x}$ and $\overrightarrow{y}$ directions

for the different Young's modulus values. As we can see the general behavior is the same between the model with skin and the model without skin. The sensitivity of the model to the skin effect decays as the foibroglandular tissue is stiffer.

We notice as expected that the stiffer is the fibroglandular tissue, the smaller is displacement. There is however a saturation effect and we get roughly the same displacement when fibroglandular are $10, 15$ and 20 times stiffer than fat.

We have tested second the effect of the presence of a small tumor on these deformations. We place some disk of 1cm radius to model a tumor and look at the impact on the deformation of the breast while the tumor is supposed to be 25 stiffer than the fat tissue. We observe mainly a local perturbation of the previous results. In particular the markers closest to the tumor get most affected as one can expect.

This sensitivity analysis reveals (with a two dimensional simulation), the importance of the choice of the breast model. An homogeneous tissue description to model the breast would be inaccurate. However regarding to the general behavior an exact description of the tissue property is not mandatory. Moreover this will lead to ex-

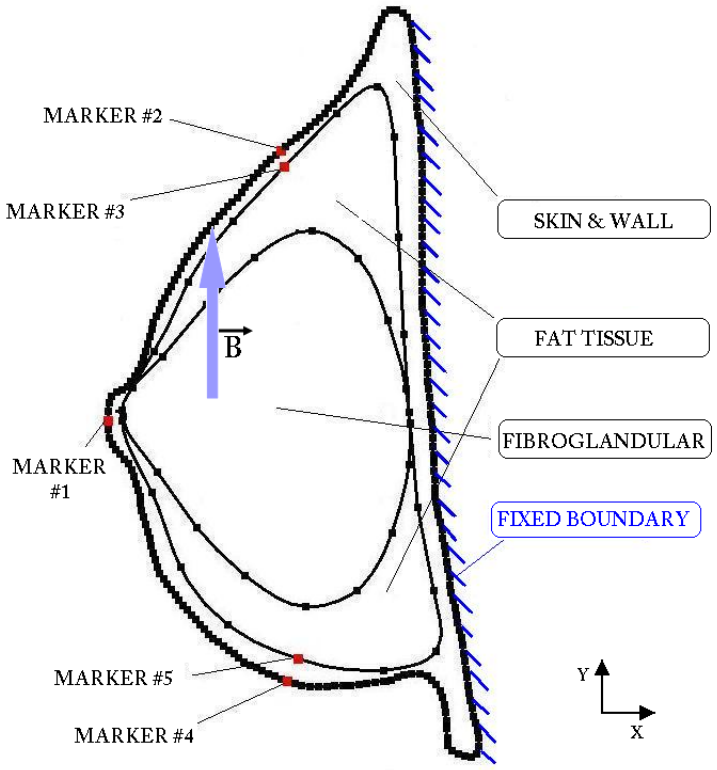

Fig. 8 Model for the sensitivity analysis of the Fibroglandular tissue.

cessive constrain at the input of our model. One speculate that a coarse distribution of the tissue is needed to have prediction that fit within a few millimeter accuracy. Regarding the skin introduction in the model, the skin affects the amplitude of displacement, however the skin introduction does not impact the general behavior of the deformation.

With three dimensional clinical data, we expect to retrieve some good tissue composition indicator with either a coarse segmentations of MRI images, or even better elastography imaging. We can expect however some uncertainty left on those tissue mechanical properties, and a practical solution would be to calibrate the mechanical

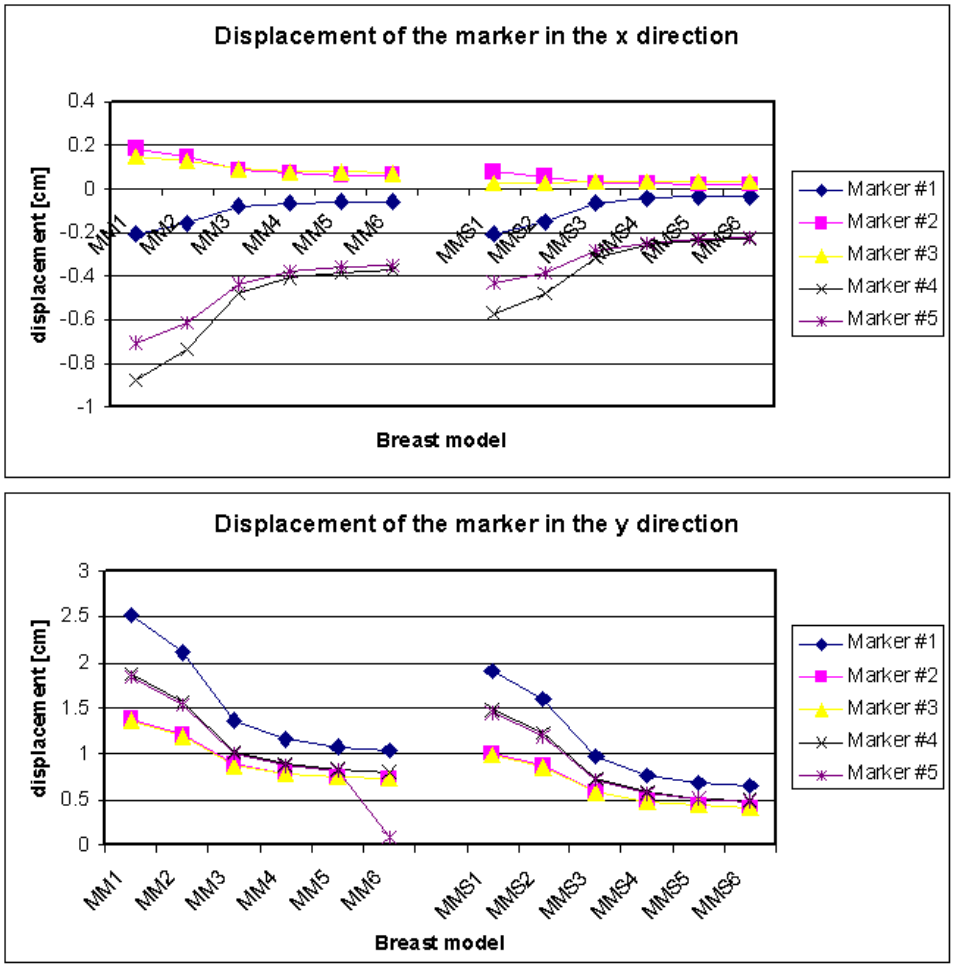

Fig. 9 Displacement of the different marker along x and y direction after loading

.

model with breast external 3d images obtained in various positions relative to the gravity. The solution of this identification problem may use the same optimization framework that the one we use for recovering the unloaded position.

3 Conclusion

The motivation of this study was to highlight the different aspects that it takes to develop a reliable mechanical model of breast deformation for BCT, in order to provide a good predictive tool for surgery. We discussed the choice of the model with linear elastic, hyperelastic approximation to simulate breast tissue and multi-material description in particular for tissue removal. We found global deformation and local deformation due to BCT with good correlation with surgeons observations. A sensitivity analysis was run to determine what are the most significant parameters to measure. We have shown that we can learn much from artificial benchmark problems and they should be used as a preliminary test of methods and ideas for BCT. However a reliable predictive model needs much more work and should start from the clinical data we have started to accumulate. Our next step will be to concentrate on a mechanical model that retain enough of the desired characteristic to predict outcomes of BCT but can still work in a clinical environment characterized by a significant level of uncertainty on tissue properties. Later on this mechanical model will be coupled to a tumor growth model that should provide information on negative margin in surgery planning.

References

1. F.S.Azar, D.N. Metaxas and M.D.Schnall, *A Finite Element Model of the Breast for Predicting Mechanical Deformations During Interventional Procedures,* Proc. Int. Soc. Magn. Reson. Med. 7, 1084, 1999.
2. F.S.Azar, D.N. Metaxas and M.D.Schnall, *Methods for Modeling and Predicting Mechanical Deformations of the Breast Under External Perturbations,* Medical Image Analysis 6, 2002, 1-27.
3. Bailey, A. M., B. C. Thorne, and S. M. Peirce, *Multi-cell agent-based simulation of the microvasculature to study the dynamics of circulating inflammatory cell trafficking,* Ann. Biomed. Eng. 35:916-936, 2007.
4. Scott A. Berceli, Roger Tran-Son-Tay, Marc Garbey, and Zhihua Jiang, *Hemo- dynamically Driven Vein Graft Remodeling: A Systems Biology Approach,* to appear in Vascular - The international Society for Vascular Surgery, Vol16, 2008.
5. Deutsch, A., and S. Dormann, *Cellular Automaton Modeling of Biological Pattern Formation,* Boston: Birkhuser, 2005.
6. Mallet, D. G., and L. G. De Pillis, *A cellular automata model of tumor-immune system interactions,* J. Theor. Biol. 239:334-350, 2006.
7. Mi, Q., B. Rivire, G. Clermont, D. L. Steed, and Y. Vodovotz. *Agent-based model of inflammation and wound healing: insights into diabetic foot ulcer pathology and the role of transforming growth factor-β1,* Wound Repair Regen. 15:671-682, 2007.

8. R.K.Benda et Al, *Breast-Conserving Therapy (BCT) for Early Stage Breast Cancer,* Journal of Surgical Oncology 2004,85:14-27.
9. Galle, J., M. Hoffmann, and G. Aust, *From single cells to tissue architecture-a bottom-up approach to modelling the spatio-temporal organisation of complex multi-cellular systems,* J. Math. Biol. 58:261-283, 2009.
10. J.H.Holland, *Hidden Order: How Adaptation Builds Complexity,* Helix Books, 1995.
11. M.H.Hwang, M.Garbey, S.C.Berceli and R. Tran Son Tay, *Ruled-Based Simulation of Multi-Cellular Biological Systems - A Revew of Modeling Technique,* xxxx
12. T.A.Krosukop et Al, *Elastic Moduli of Breast and Prostate Tissues Under Compression,* Ultrasonic Imaging 20, 260-274, 1998.
13. A.Manduca et al, *Magnetic Resonance Elastography: Non-Invasive Mapping of Tissue Elasticity,* Medical Image Analysis 5, 2001, 237-254.
14. V.Rajagopal, J.H.Chung, D.Bullivant, P.M.F.Nielsen and M.P.Nash, *Determining the Finite Elasticity Reference State From a Loaded Configuration,* Int. J. for Num. Method. in Engng, 2007 72: 1434-1451.
15. V.Rajagopal, A.Lee, et al, *Creating Individual-Specific Biomechanical Models of the Breast for Medical Image Analysis,* Acad Radiol 2008, 15:1425-1436.
16. J.Sciaretta, J.Bishop, A. Samani, D.B.Plewes, *MR Validation of Soft Tissue Deformation as Modeled by Non-Linear Finite Element Analysis,* Proc. Int. Soc. Magn. Reson. Med. 7, 246, 1999.
17. R.Sivaramakrishna, *3D Breast Image Registration - AReview,* Tecnol Cancer Res Treatment 2005, 4-39-48.
18. C.Tanner, J.Schnabel, D.Hill et al, *Factors influencing the accuracy of biomechanical models,* Med Phys. J. 2006; 33:1758-1769.
19. Thorne, B. C., A. M. Bailey, and S. M. Peirce, *Combining experiments with multi-cell agent-based modeling to study biological tissue patterning,* Brief Bioinform. 8:245-257, 2007.
20. C.Williams, B.Clymer, P.Schmalbrock, Biomechanics of Breast Tissue: Preliminary Study of Force-Deformation Relationship, Proc. Int. Soc. Magn. Reson. Med. 7, 524, 1999.
21. S.Wolfram, *Cellular Automata and Complexity, collected papers,* Westview Press 1994.
22. Schwartz Jean-Marc, *Calcul rapide de forces et de deformations mecaniques non-lineaires et visco-elastiques pour la simulation de chirurgie* University Laval Ph.D. 2003.
23. COMSOL 3.4, COMSOL Multiphysics, COMSOL Reaction Engineering Lab